

Entropic uncertainty relation in Garfinkle-Horowitz-Strominger dilation black hole

Soroush Haseli^{a,1}, Hazhir Dolatkhan², Shahryar Salimi²

¹Faculty of physics, Urmia university of technology, Urmia, Iran

²Department of Physics, University of Kurdistan, P.O.Box 66177-15175, Sanandaj, Iran

Received: date / Accepted: date

Abstract Heisenberg's uncertainty principle is a fundamental element in quantum mechanics. It sets a bound on our ability to predict the measurement outcomes of two incompatible observables, simultaneously. In quantum information theory, the uncertainty principle can be expressed using entropic measures. The entropic uncertainty relation can be improved by considering an additional particle as a memory particle. The presence of quantum correlation between the memory particle and the measured particle reduces the uncertainty. In a curved space-time the presence of the Hawking radiation can reduce quantum correlation. So, with regard to the relation between the quantum correlation and entropic uncertainty lower bound, we expect that the Hawking radiation increases the entropic uncertainty lower bound. In this work we investigate the entropic uncertainty relation in Garfinkle-Horowitz-Strominger (GHS) dilation black hole. We consider a model in which the memory particle is located near the event horizon outside the black hole, while the measured particle is free falling. To study the proposed model, we will consider examples with Dirac fields. We also explore the effect of the Hawking radiation on quantum secret key rate.

1 Introduction

The uncertainty principle is one of the distinguishing features between quantum and classical theory. The Heisenberg uncertainty principle states that it is not possible to accurately measure the location and momentum of a particle accurately [1]. Accurate measurement of one observable reduces the accuracy of another observable measurement. So far, this principle has been

expressed in various ways. One of the most fundamental forms of expressing the uncertainty principle is provided by Schrodinger [2] and Robertson [3]. They showed that for any arbitrary pairs of noncommuting observables Q and R the following relation is established for uncertainty principle

$$\Delta Q \Delta R \geq \frac{1}{2} |\langle [Q, R] \rangle|, \quad (1)$$

where $\Delta X = \sqrt{\langle X^2 \rangle - \langle X \rangle^2}$ with $X \in \{Q, R\}$ is the standard deviation of the associated observable X , $\langle X \rangle$ shows the expectation value of operator X and $[Q, R] = QR - RQ$. The lower bound in Eq.(1) is state dependent which leads to a trivial bound if $|\langle [Q, R] \rangle| = 0$. In quantum information theory, it has been shown that the most appropriate quantity to show the uncertainty is entropy. Uncertainty relations that are defined in terms of entropy are called entropic uncertainty relation (EUR). The first EUR was speculated by Deutsch [4], then improved by Kraus [5], and finally proved by Maassen and Uffink [6]. They showed that for any arbitrary pairs of observables Q and R EUR can be written as

$$H(Q) + H(R) \geq \log_2 \frac{1}{c} \quad (2)$$

where $H(Q) = -\sum_i p_i \log_2 p_i$ and $H(R) = -\sum_j m_j \log_2 m_j$ are the Shannon entropy, $p_i = \langle q_i | \rho | q_i \rangle$, $m_j = \langle r_j | \rho | r_j \rangle$ and $c = \max_{i,j} \{ |\langle q_i | r_j \rangle|^2 \}$ where $|q_i\rangle$ and $|r_j\rangle$ are eigenstates of observables Q and R , respectively. This statement of uncertainty principle can be described by an interesting game between Alice and Bob. At the beginning of the game, Bob prepares the particle in a quantum state ρ and sends it to Alice. In the second step, Alice and Bob agree on the measurement of two observables Q and R by Alice on the particle. Then

^ae-mail: soroush.haseli@uut.ac.ir

Alice measures one of the two observable Q or R on her state and sends her measurement choice to Bob via a classical communication channel. If Bob guesses Alice's measurement correctly, he will win the game. The Bob's uncertainty about Alice's measurement outcomes is bounded by Eq.(2). In this statement of the uncertainty principle, there was only one particle. But when Bob prepares a correlated bipartite state ρ_{AB} for two particle quantum system and sends one of the particles to Alice and keeps the other part as a quantum memory, he can guess the result of Alice's measurement more accurately. Based on this uncertainty game, Berta et al. have presented the EUR in the presence of quantum memory *EUR-QM) as [7]

$$S(Q|B) + S(R|B) \geq \log_2 \frac{1}{c} + S(A|B), \quad (3)$$

where $S(Q|B) = S(\rho^{QB}) - S(\rho^B)$ and $S(R|B) = S(\rho^{RB}) - S(\rho^B)$ are the conditional von-Neumann entropies of the post measurement states

$$\begin{aligned} \rho^{QB} &= \sum_i (|q_i\rangle\langle q_i| \otimes I) \rho^{AB} (|q_i\rangle\langle q_i| \otimes I), \\ \rho^{RB} &= \sum_j (|r_j\rangle\langle r_j| \otimes I) \rho^{AB} (|r_j\rangle\langle r_j| \otimes I), \end{aligned} \quad (4)$$

and $S(A|B) = S(\rho^{AB}) - S(\rho^B)$ is the conditional von Neumann entropy. Let's take a look at some special cases: At first, If particles A and B are entangled, the conditional von-Neumann entropy is negative and Bob can guess the result of Alice's measurement with better accuracy. Second, If Bob prepares the maximally entangled state in uncertainty game then Bob can guess the result of Alice's measurement perfectly [7]. Third, If there is no memory particle, then from Eq.(3), the EUR is obtained as

$$H(Q) + H(R) \geq \log_2 \frac{1}{c} + S(A). \quad (5)$$

Due to the presence of an additional term $S(A)$, the above EUR is tighter than Maassen and Uffink uncertainty relation. So far, several works have been done to improve the EUR [8–66]. In Ref. [62], the authors introduced a new bound for the EUR-QM. They showed that the Bob's uncertainty about the results of Alice's measurement is bounded by

$$\begin{aligned} S(Q|B) + S(R|B) &= \\ &= H(Q) - I(Q; B) + H(R) - I(R; B) \\ &\geq \log_2 \frac{1}{c} + S(A) - [I(Q; B) + I(R; B)] \\ &= \log_2 \frac{1}{c} + S(A|B) + \\ &+ \{I(A; B) - [I(Q; B) + I(R; B)]\}. \end{aligned} \quad (6)$$

Based on their results the EUR-QM can be written as

$$S(Q|B) + S(R|B) \geq \log_2 \frac{1}{c} + S(A|B) + \max\{0, \delta\} \quad (7)$$

where

$$\delta = I(A; B) - (I(Q; B) + I(R; B)) \quad (8)$$

and

$$I(X; B) = S(\rho^B) - \sum_x p_x S(\rho_x^B), \quad X \in \{Q, R\}, \quad (9)$$

Eq.9 is known as Holevo quantity, $p_x = \text{tr}_{AB}(\Pi_x^A \rho^{AB} \Pi_x^A)$ is the probability of x-th outcome and $\rho_x^B = \frac{\text{tr}_A(\Pi_x^A \rho^{AB} \Pi_x^A)}{p_x}$ is the Bob's state after the measurement of X by Alice. It is worth noting that the EUR is tighter than other EURs in the presence of quantum memory.

The EUR has a variety of applications in quantum information theory such as entanglement detection [67–70], and quantum cryptography [71, 72]. The security of quantum key distribution protocols can be verified using the EURs [73, 74]. It has been shown that the bound of EUR-QM is directly related to the quantum secret key (QSK) rate [66, 75]. In Ref. [66], the authors have shown that the amount of key that can be extracted by Alice and Bob K is lower bounded as

$$K \geq \log_2 \frac{1}{c} + \max\{0, \delta\} - S(R|B) - S(Q|B), \quad (10)$$

The study of the EUR-QM from a relativistic point of view has been the subject of some recent works [76–79]. What is clear is that the entropic uncertainty bound decreases with increasing quantum correlation between the measured particle A and the quantum memory B . In Refs.[80–84], the authors have shown that the quantum correlation decreases under the influence of Hawking radiation and so the entropic uncertainty increases. In order to study the effects of Hawking radiation on entropic uncertainty bound, we consider the simplest black hole: Garfinkle-Horowitz-Strominger (GHS) dilation black hole. We also consider the Dirac fields states as the examples. In this situation, a quantum state is a combination of vacuum state and excited states of Dirac fields. In GHS dilation black hole space-time we will consider a model in which the memory particle B is located somewhere near the event horizon outside the black hole and the measured particle A is free falling. When the memory particle gets closer to the event horizon the entanglement between particle memory B and measured particle A decreases due to Unruh effect. In such a situation, the lower bound of EUR-QM increases with decreasing entanglement. This article is organized as follows.

2 Quantum channel interpretation of the vacuum structure for Dirac fields in the GHS dilation black hole

In Refs. [85, 86], the thermal Fermi-Dirac distribution of particles with the Hawking temperature $T = \frac{1}{8\pi(M-D)}$ has been investigated in GHS dilation black hole [87]. The existence of such radiation has been described as the Hawking effect. The cosmological parameters M and D represent the mass of the black hole and dilation field, respectively. Here, according to the Dirac vacuum field in GHS dilation black hole, the global coordinates (t, r, θ, ϕ) is used to represent the spherically symmetric line element of the GHS dilation black hole [88–90]

$$ds^2 = - \left(\frac{r-2M}{r-2D} \right) dt^2 + \left(\frac{r-2M}{r-2D} \right)^{-1} dr^2 + r(r-2D) (d\theta^2 + \sin^2 \theta d\phi^2). \quad (11)$$

Throughout this paper the natural units are set as $\hbar = G = c = k_B = 1$. The massless Dirac equation can be written as $\gamma^\alpha e_a^\mu (\partial_\mu + \Gamma_\mu) \psi = 0$, where γ^α is Dirac matrix, e_a^μ corresponds to the inverse of the tetrad and Γ_μ is the spin connection coefficient. Solving massless Dirac equation near the event horizon leads to positive frequency outgoing solutions outside region I and inside regions II as [88]

$$\psi_k^{\nu+} = \xi e^{\mp i\omega u}, \quad (12)$$

where $\nu \in \{I, II\}$ shows the regions, k represents the field mode, ξ is a 4-component Dirac spinor and ω is a monochromatic frequency of the Dirac field. In Eq. (12), u represents the retarded time and is defined as follows

$$u = t - 2(M-D) \ln \left[\frac{r-2M}{2M-2D} \right]. \quad (13)$$

To show the general form of the GHS dilation black hole, the Carter-Penrose diagrams for this space-times is plotted in Fig. 1. In diagram $r = 2M$ shows the event horizons and $r = 2D$ represents the singularity of the black hole. I and II show the two general disconnected regions. The Dirac field can be quantized by using the complete orthogonal basis $\psi_k^{\nu+}$ as

$$\psi_{\text{out}} = \sum_{\nu=I,II} \int dk (a_k^\nu \psi_k^{\nu+} + b_k^{\nu*} \psi_k^{\nu-}) \quad (14)$$

where a_k^ν and $b_k^{\nu*}$ are the fermion annihilation and antifermion creation operators respectively. One can use the generalized Kruskal coordinates to introduce new orthogonal basis for positive energy mode as

$$\begin{aligned} \chi_k^{I+} &= e^{2(M-D)\pi\omega} \psi_k^{I+} + e^{-2(M-D)\pi\omega} \psi_{-k}^{II-}, \\ \chi_k^{II+} &= e^{-2(M-D)\pi\omega} \psi_{-k}^{I-} + e^{2(M-D)\pi\omega} \psi_k^{II+}. \end{aligned} \quad (15)$$

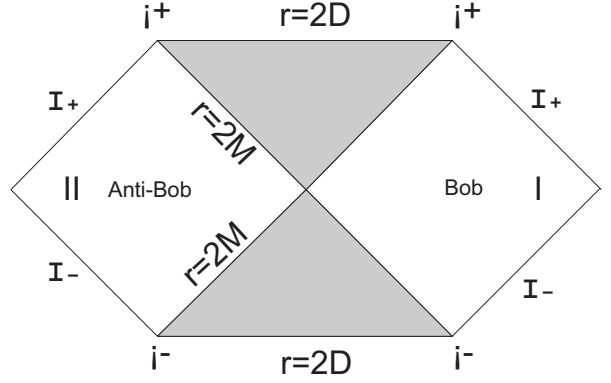


Fig. 1 The Penrose diagrams for the GHS dilation black hole which shows the world-line of Bob and Anti-Bob. i_0 denotes the spatial infinities, i (i^+) represents time-like past (future) infinity. I_- (I_+) shows light-like past (future) infinity.

These new bases can be used to expand the Dirac fields in the Kruskal coordinates as

$$\begin{aligned} \psi_{\text{out}} &= \sum_{\nu=I,II} \int dk \left| \frac{1}{\sqrt{2 \cosh[4(M-D)\pi\omega]}} \right. \\ &\quad \times (c_k^\nu \chi_k^{\nu+} + d_k^{\nu*} \chi_k^{\nu-}), \end{aligned} \quad (16)$$

where c_k^ν and $d_k^{\nu*}$ are the fermion annihilation and antifermion creation operators which act on the Kruskal vacuum. Eq. (14) is the expansion of Dirac field in GHS dilation while Eq. (16) corresponds to the decomposition of Dirac field in Kruskal modes. Using a suitable Bogoliubov transformation, one can obtain the annihilation operator c_k^ν as

$$c_k^I = (e^{-\frac{\omega}{T}} + 1)^{-\frac{1}{2}} a_k^I - (e^{\frac{\omega}{T}} + 1)^{-\frac{1}{2}} b_k^{II*} \quad (17)$$

where T is the radiation temperature [91–93]. The form of ground state in the GHS dilation coordinates is regarded as a two-mode squeezed state in Kruskal coordinates. So, the vacuum and excited state can be expanded as follows

$$\begin{aligned} |0\rangle^+ &= x^{-\frac{1}{2}} |0\rangle_I^+ |0\rangle_{II}^- + y^{-\frac{1}{2}} |1\rangle_I^+ |1\rangle_{II}^- \\ |1\rangle^+ &= |1\rangle_I^+ |0\rangle_{II}^- \end{aligned} \quad (18)$$

where $x = (e^{-\frac{\omega}{T}} + 1)$, $y = (e^{\frac{\omega}{T}} + 1)$, $|n\rangle_I$ and $|n\rangle_{II}$ are the orthonormal basis of outside and inside region of the event horizon respectively. The superscripts $+$ and $-$ show the particle and anti-particle respectively. In the following, we abandon the superscripts \pm in order to simplify the formulation. Since the region I and II are completely disconnected, one can obtain the physical accessible part I by tracing over the state of the region II . Interestingly, the whole process can be thought of as a quantum channel [91]. In dynamics of open quantum system, the state of the system changes as a result of interaction with its surroundings. So, loss of information

in space-time with the event horizon can be considered as an open quantum system. Changing the state of an open quantum system at a given time is described by a dynamical map or quantum channel. The dynamical map Φ_t converts the initial state of the system ρ_0 to the evolved state ρ_t as $\rho_0 \rightarrow \rho_t = \Phi_t \rho_0$. The dynamical map can be written in Kraus form as $\rho_t = \Phi_t \rho_0 = \sum_m W_m \rho_0 W_m^\dagger$. If the initial state of the system is considered as $\rho_0 = \sum_{i,j=0,1} \rho_{ij} |i\rangle\langle j|$, the dynamical map can be written as $\Phi_t \rho_0 = \sum_{i,j=0,1} \varepsilon(|i\rangle\langle j|) \rho_{ij}$, where $\varepsilon(|i\rangle\langle j|) = \sum_m W_m (|i\rangle\langle j|) W_m^\dagger$. Considering the GHS dilation black hole, the dynamical map can be written as the Unruh channel,

$$\begin{aligned} \varepsilon(|0\rangle\langle 0|) &= (e^{-\frac{\omega}{T}} + 1)^{-1} |0\rangle_I\langle 0| + (e^{\frac{\omega}{T}} + 1)^{-1} |1\rangle_I\langle 1| \\ \varepsilon(|0\rangle\langle 1|) &= (e^{-\frac{\omega}{T}} + 1)^{-\frac{1}{2}} |0\rangle_I\langle 1| \\ \varepsilon(|1\rangle\langle 0|) &= (e^{-\frac{\omega}{T}} + 1)^{-\frac{1}{2}} |1\rangle_I\langle 0| \\ \varepsilon(|1\rangle\langle 1|) &= |1\rangle_I\langle 1|, \end{aligned} \quad (19)$$

where the partial trace is done over the state of the interior region. In Fig.2(a), the entropic uncertainty lower bound is plotted in terms of probability parameter p for different value of Hawking temperature. As can be seen the entropic uncertainty lower bound increases with increasing Hawking temperature. This is what we expected, the quantum correlation decreases under the influence of Hawking radiation and so the entropic uncertainty increases with increasing Hawking temperature [80–84]. Fig.2(b) shows the contour plot of entropic uncertainty lower bound in terms of Hawking temperature T and probability parameter p . As can be seen from Fig.2(b), at different Hawking temperatures the the entropic uncertainty lower bound has its lowest value for the case in which $p = 1$ and the state is maximally entangled. It is also observed that for different values of p this entropic uncertainty lower bound increases with increasing Hawking temperature.

3 Entropic uncertainty lower bound in Garfinkle-Horowitz-Strominger dilation black hole

In this section the uncertainty game between Alice and Bob in Garfinkle-Horowitz-Strominger dilation black hole is investigated. At the beginning of the game, Bob prepares a correlated bipartite state ρ_{AB} then sends the first part to Alice and keeps the other part as a quantum memory. In this step of the game, both of them free falling towards the black hole. In the next step, Alice remains free falling into the black hole while Bob is

in a fixed position outside the black hole. Then Alice measures one of the two observable Q or R on her state and sends her measurement choice to Bob via a classical communication channel. The main purpose of this game for Bob is to reduce his uncertainty about the result of Alice's measurement. If Bob can correctly guess the result of Alice's measurement in this situation, he will win this game. Due to the fact that the resident observer cannot access modes beyond the event horizon, the lost information reduces the entanglement between Alice and Bob. So, it changes the uncertainty bound. By reducing Bob's distance from the black hole's event horizon, his uncertainty about the result of Alice's measurement will increase.

4 Examples

4.1 Bell diagonal state

As a first example, let us consider the case in which Alice and Bob share the set of two-qubit states with the maximally mixed marginal states. This state is defined as follows

$$\rho^{AB} = \frac{1}{4} \left(I \otimes I + \sum_{i=1}^3 w_{ij} \sigma_i \otimes \sigma_j \right) \quad (20)$$

where $\sigma_i (i = 1, 2, 3)$ are the Pauli matrices. Using the singular value decomposition, the matrix $W = \{w_{ij}\}$ can be diagonalized by a local unitary transformation. So, Eq. (20) can be rewritten as

$$\rho^{AB} = \frac{1}{4} (I \otimes I + \sum_i r_i \sigma_i \otimes \sigma_i), \quad (21)$$

where $\mathbf{r} = (r_1, r_2, r_3)$ is limited to a tetrahedron defined by the set of vertices $(-1, -1, -1)$, $(-1, 1, 1)$, $(1, -1, 1)$ and $(1, 1, -1)$. We consider the case in which $r_1 = 1 - 2p$, $r_2 = -p$ and $r_3 = -p$ where $0 \leq p \leq 1$. So the state in Eq.(22) can be written as

$$\rho^{AB} = p |\Psi^-\rangle\langle\Psi^-| + \frac{1-p}{2} (|\Psi^+\rangle\langle\Psi^+| + |\Phi^+\rangle\langle\Phi^+|), \quad (22)$$

where $|\Psi^\pm\rangle = \frac{1}{\sqrt{2}}(|01\rangle \pm |10\rangle)$ and $|\Phi^\pm\rangle = \frac{1}{\sqrt{2}}(|00\rangle \pm |11\rangle)$. We consider a model in which the memory particle B (At the disposal of Bob) is located near the event horizon outside the black hole, while the measured particle A (At the disposal of Alice) is free falling. The effect of Hawking radiation can be defined by applying the Unruh channel in Eq.(19) on Bob's state.

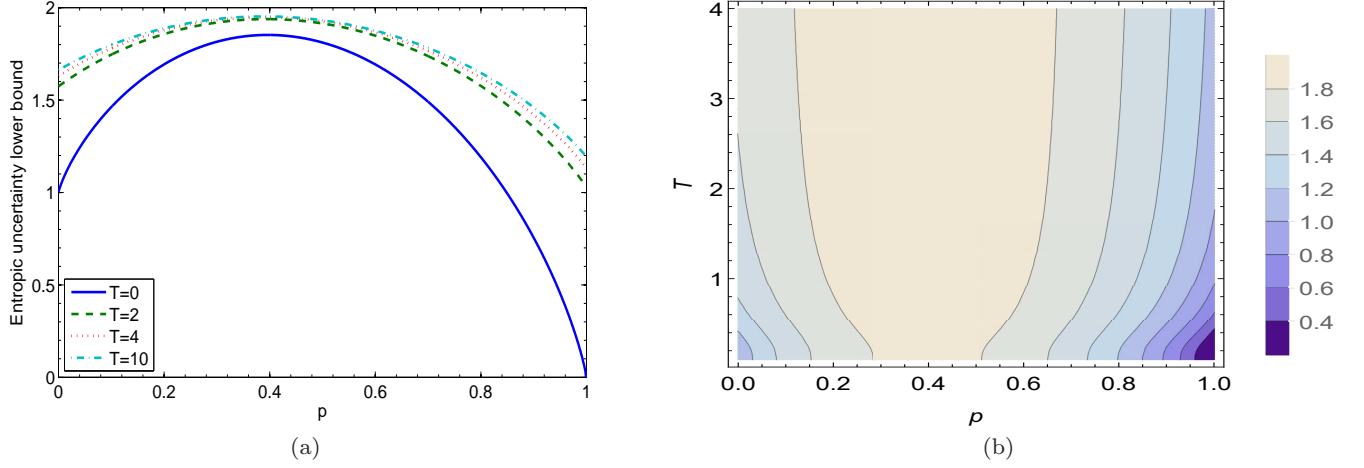


Fig. 2 (a) Entropic uncertainty lower bound when Bob prepare a correlated bipartite state in a special class of state: $\rho^{AB} = p|\Psi^-\rangle\langle\Psi^-| + \frac{1-p}{2}(|\Psi^+\rangle\langle\Psi^+| + |\Phi^+\rangle\langle\Phi^+|)$ in terms of probability parameter p for different value of Hawking temperature when $\omega = 1$. (b) The contour plot of entropic uncertainty lower bound when Bob prepare a correlated bipartite state in a special class of state: $\rho^{AB} = p|\Psi^-\rangle\langle\Psi^-| + \frac{1-p}{2}(|\Psi^+\rangle\langle\Psi^+| + |\Phi^+\rangle\langle\Phi^+|)$ in terms of Hawking temperature T and probability parameter p when $\omega = 1$.

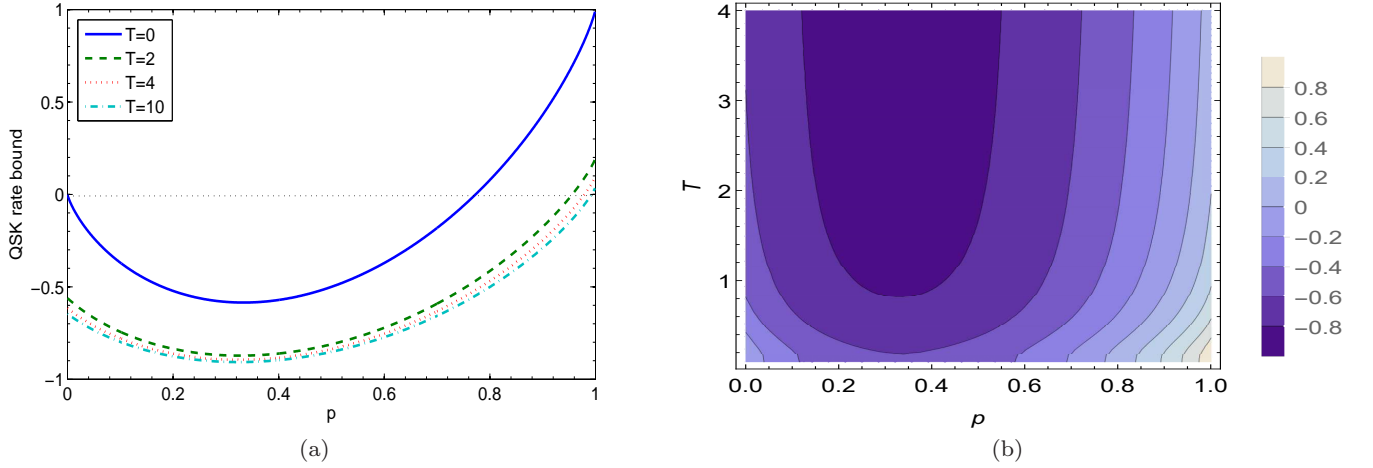


Fig. 3 (a) QSK rate bound when Bob prepare a correlated bipartite state in a special class of state: $\rho^{AB} = p|\Psi^-\rangle\langle\Psi^-| + \frac{1-p}{2}(|\Psi^+\rangle\langle\Psi^+| + |\Phi^+\rangle\langle\Phi^+|)$ in terms of probability parameter p for different value of Hawking temperature when $\omega = 1$. (b) The contour plot of QSK rate bound when Bob prepare a correlated bipartite state in a special class of state: $\rho^{AB} = p|\Psi^-\rangle\langle\Psi^-| + \frac{1-p}{2}(|\Psi^+\rangle\langle\Psi^+| + |\Phi^+\rangle\langle\Phi^+|)$ in terms of Hawking temperature T and probability parameter p when $\omega = 1$.

In Fig.3(a), the QSK rate bound is plotted in terms of probability parameter p for different value of Hawking temperature. As can be seen the QSK rate bound decreases with increasing Hawking temperature. This is what we expected, the quantum correlation decreases under the influence of Hawking radiation and so the QSK rate decreases with increasing Hawking temperature. Fig.3(b) shows the contour plot of QSK rate bound in terms of Hawking temperature T and probability parameter p . As can be seen from Fig.3(b), at dif-

ferent Hawking temperatures the the QSK rate bound has its highest value for the case in which $p = 1$ and the state is maximally entangled. It is also observed that for different values of p the QSK rate bound decreases with increasing Hawking temperature. As can be seen from Figs.3(a) and 3(b), the QSK rate bounds is negative for some values of p and T . So, one can concluded that for these values of p and T the states are not good enough to support quantum key distribution protocols.

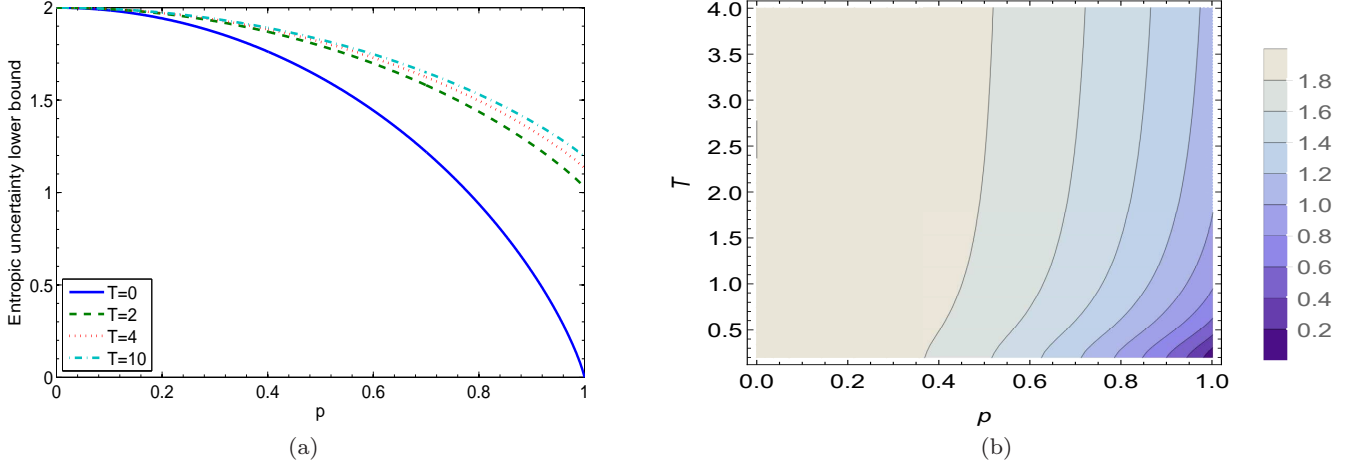


Fig. 4 (a) Entropic uncertainty lower bound when Bob prepare a correlated bipartite state in a special class of state: $\rho^{AB} = \frac{1-p}{4}I \otimes I + p|\psi^-\rangle\langle\psi^-|$ in terms of probability parameter p for different value of Hawking temperature when $\omega = 1$. (b) The contour plot of entropic uncertainty lower bound when Bob prepare a correlated bipartite state in a special class of state: $\rho^{AB} = \frac{1-p}{4}I \otimes I + p|\psi^-\rangle\langle\psi^-|$ in terms of Hawking temperature T and probability parameter p when $\omega = 1$.

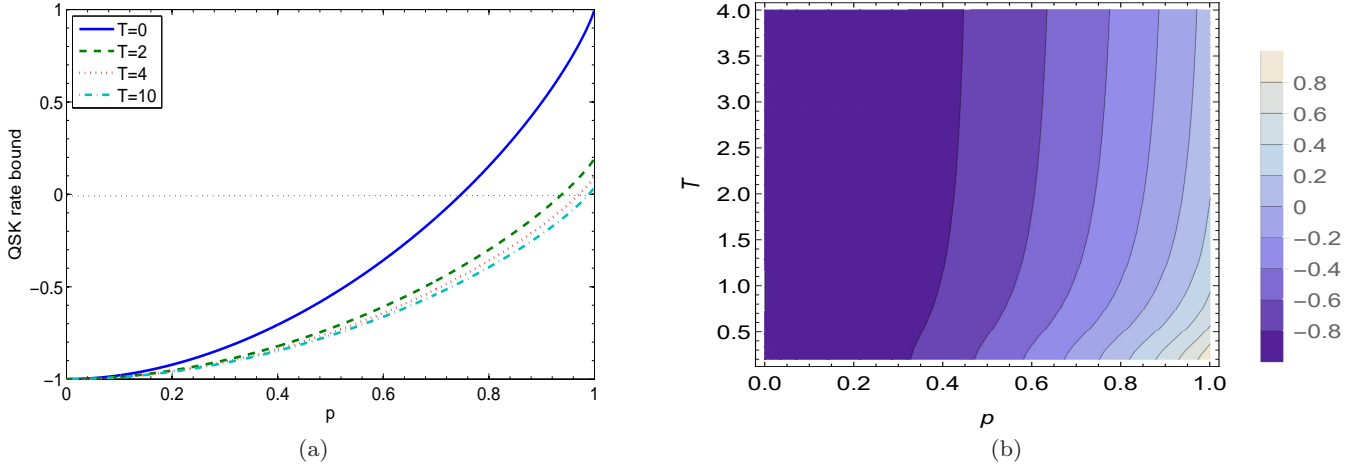


Fig. 5 (a) QSK rate bound when Bob prepare a correlated bipartite state in a special class of state: $\rho^{AB} = \frac{1-p}{4}I \otimes I + p|\psi^-\rangle\langle\psi^-|$ in terms of probability parameter p for different value of Hawking temperature when $\omega = 1$. (b) The contour plot of QSK rate bound when Bob prepare a correlated bipartite state in a special class of state: $\rho^{AB} = \frac{1-p}{4}I \otimes I + p|\psi^-\rangle\langle\psi^-|$ in terms of Hawking temperature T and probability parameter p when $\omega = 1$.

4.2 Werner state

As a second example, Let us consider the case in which Alice and Bob initially share a two-qubit Werner state

$$\rho^{AB} = \frac{1-p}{4}I \otimes I + p|\psi^-\rangle\langle\psi^-|, \quad (23)$$

where $0 \leq p \leq 1$.

In Fig.4(a), the entropic uncertainty lower bound is plotted in terms of probability parameter p for different value of Hawking temperature. As can be seen the entropic uncertainty lower bound increases with in-

creasing Hawking temperature. Fig.4(b) shows the contour plot of entropic uncertainty lower bound in terms of Hawking temperature T and probability parameter p . As can be seen from Fig.4(b), at different Hawking temperatures the the entropic uncertainty lower bound has its lowest value for the case in which $p = 1$ and the state is maximally entangled. It is observed that for different values of p this entropic uncertainty lower bound increases with increasing Hawking temperature. It is also observed that for the case in which $p = 0$,

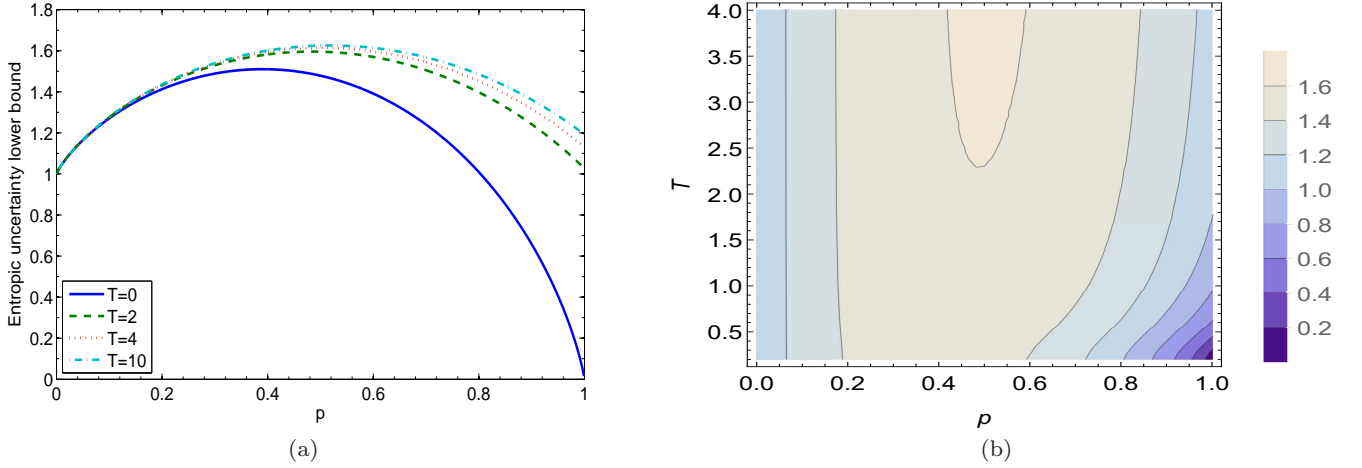


Fig. 6 (a) Entropic uncertainty lower bound when Bob prepare a correlated bipartite state in a special class of state: $\rho^{AB} = p|\Psi^+\rangle\langle\Psi^+| + (1-p)|11\rangle\langle 11|$ in terms of probability parameter p for different value of Hawking temperature when $\omega = 1$. (b) The contour plot of entropic uncertainty lower bound when Bob prepare a correlated bipartite state in a special class of state: $\rho^{AB} = p|\Psi^+\rangle\langle\Psi^+| + (1-p)|11\rangle\langle 11|$ in terms of Hawking temperature T and probability parameter p when $\omega = 1$.

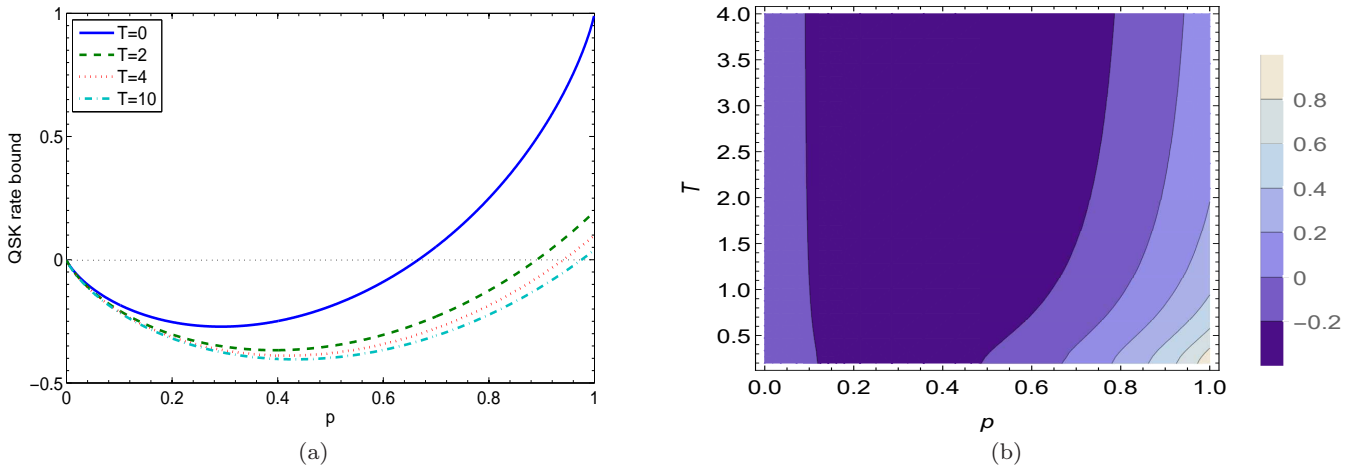


Fig. 7 (a) QSK rate bound when Bob prepare a correlated bipartite state in a special class of state: $\rho^{AB} = \frac{1-p}{4}I \otimes I + p|\psi^-\rangle\langle\psi^-|$ in terms of probability parameter p for different value of Hawking temperature when $\omega = 1$. (b) The contour plot of QSK rate bound when Bob prepare a correlated bipartite state in a special class of state: $\rho^{AB} = \frac{1-p}{4}I \otimes I + p|\psi^-\rangle\langle\psi^-|$ in terms of Hawking temperature T and probability parameter p when $\omega = 1$.

the entropic uncertainty lower bound not affected by Hawking radiation.

In Fig.5(a), the QSK rate bound is plotted in terms of probability parameter p for different value of Hawking temperature. As can be seen the QSK rate bound decreases with increasing Hawking temperature. This is what we expected, the quantum correlation decreases under the influence of Hawking radiation and so the QSK rate decreases with increasing Hawking temperature. Fig.5(b) shows the contour plot of QSK rate bound in terms of Hawking temperature T and proba-

bility parameter p . As can be seen from Fig.5(b), at different Hawking temperatures the the QSK rate bound has its highest value for the case in which $p = 1$ and the state is maximally entangled. It is also observed that for different values of p the QSK rate bound decreases with increasing Hawking temperature. As can be seen from Figs.5(a) and 5(b), the QSK rate bounds is negative for some values of p and T . So, one can concluded that for these values of p and T the states are not good enough to support quantum key distribution protocols. It is also observed that for the case in which

$p = 0$, the QSK rate bound not affected by Hawking radiation.

4.3 Two-qubit X states

As the last example, let us consider the case in which Alice and Bob share a special class of two qubit X states

$$\rho^{AB} = p|\Psi^+\rangle\langle\Psi^+| + (1-p)|11\rangle\langle 11|, \quad (24)$$

where $0 \leq p \leq 1$.

In Fig.6(a), the entropic uncertainty lower bound is plotted in terms of probability parameter p for different value of Hawking temperature. The entropic uncertainty lower bound increases with increasing Hawking temperature. Fig.6(b) shows the contour plot of entropic uncertainty lower bound in terms of Hawking temperature T and probability parameter p . As can be seen from Fig.6(b), at different Hawking temperatures the the entropic uncertainty lower bound has its lowest value for the case in which $p = 1$ and the state is maximally entangled. It is observed that for different values of p this entropic uncertainty lower bound increases with increasing Hawking temperature. It is also observed that for the case in which $p = 0$, the entropic uncertainty lower bound not affected by Hawking radiation.

In Fig.7(a), the QSK rate bound is plotted in terms of probability parameter p for different value of Hawking temperature. As can be seen the QSK rate bound decreases with increasing Hawking temperature. This is what we expected, the quantum correlation decreases under the influence of Hawking radiation and so the QSK rate decreases with increasing Hawking temperature. Fig.7(b) shows the contour plot of QSK rate bound in terms of Hawking temperature T and probability parameter p . As can be seen from Fig.7(b), at different Hawking temperatures the the QSK rate bound has its highest value for the case in which $p = 1$ and the state is maximally entangled. It is also observed that for different values of p the QSK rate bound decreases with increasing Hawking temperature. As can be seen from Figs.7(a) and 7(b), the QSK rate bounds is negative for some values of p and T . So, one can concluded that for these values of p and T the states are not good enough to support quantum key distribution protocols. It is also observed that for the case in which $p = 0$, the QSK rate bound not affected by Hawking radiation.

5 Conclusion

In this work we studied the entropic uncertainty relation in Garfinkle-Horowitz-Strominger dilation black hole. For this purpose, we consider the uncertainty game between Alice and Bob. At first Bob prepares a correlated bipartite state ρ_{AB} then he sends the first part A to Alice and keeps the other part as a quantum memory B . In this step of the game, both of them free falling towards the black hole. In the next step, Alice remains free falling into the black hole while Bob is in a fixed position outside the black hole. Then Alice measures one of the two observable Q or R on her state and sends her measurement choice to Bob via a classical communication channel. The main purpose of this game for Bob is to reduce his uncertainty about the result of Alice's measurement. As mentioned before, quantum correlations are reduced by the effect of Hawking radiation. Therefore, due to the inverse relation between quantum correlation and uncertainty the Uncertainty bound will increase as a result of Hawking effect. We also investigated the effects of Hawking radiation on QSK rate bound. It was shown that the QSK rate bound decreases by increasing Hawking temperature.

References

1. W. Heisenberg, Z. Phys. 43, 172 (1927).
2. E. Schrodinger, Proc. Pruss. Acad. Sci. XIX, 296 (1930).
3. H. P. Robertson, Phys. Rev. 34, 163 (1929).
4. D. Deutsch, Phys. Rev. Lett. 50 631-633 (1983).
5. K. Kraus, Phys. Rev. D 35, 3070 (1987).
6. H. Maassen and J. B. M. Uffink, Phys. Rev. Lett. 60, 1103 (1988).
7. M. Berta, M. Christandl, R. Colbeck, J. M. Renes and R. Renner, Nature Phys. 6, 659 (2010).
8. I. Bialynicki-Birula, Phys. Rev. A 74, 052101 (2006)
9. S. Wehner and A. Winter, New J. Phys. 12, 025009 (2010).
10. M. Berta, M. Christandl, R. Colbeck, J. M. Renes and R. Renner, Nature Phys. 6, 659 (2010).
11. A. K. Pati, M. M. Wilde, A. R. Usha Devi, A. K. Rajagopal and Sudha, Phys. Rev. A 86, 042105 (2012).
12. M. A. Ballester and S. Wehner, Phys. Rev. A 75, 022319 (2007).
13. J. I. De Vicente and J. Sanchez-Ruiz, Phys. Rev. A 77, 042110 (2008).
14. S. Wu, S. Yu and K. Molmer, Phys. Rev. A 79, 022104 (2009).

15. L. Rudnicki , S. P. Walborn and F. Toscano Phys. Rev. A 85, 042115 (2012).
16. T. Pramanik , P. Chowdhury and A. S. Majumdar Phys. Rev. Lett. 110, 020402 (2013).
17. L. Maccone and A. K. Pati, Phys. Rev. Lett. 113, 260401 (2014).
18. P. J. Coles and M. Piani, Phys. Rev. A 89, 022112 (2014).
19. S. Zozor , G. M. Bosyk and M. Portesi, J. Phys. A: Math. Theor. 47, 495302 (2014).
20. L. Rudnicki , Z. Puchala and K. Zyczkowski, Phys. Rev. A 89, 052115 (2014).
21. S. Liu , L. Z. Mu and H. Fan, Phys. Rev. A 91, 042133 (2015).
22. K. Korzekwa , M. Lostaglio , D. Jennings and T. Rudolph, Phys. Rev. A 89 042122 (2014).
23. L. Rudnicki, Phys. Rev. A 91, 032123 (2015).
24. J. Zhang , Y. Zhang and C. S. Yu, Sci Rep. 5, 11701 (2015).
25. T. Pramanik , S. Mal and A. S. Majumdar, Quantum Inf. Process. 15, 981 (2016).
26. Lv W M, Zhang C, Hu X M, Huang Y F, Cao H, Wang J, Hou Z B, Liu B H, Li C F and Guo G C 2019 Sci. Rep. 9 8748
27. M. L. Hu and H. Fan Phys. Rev. A 88, 014105 (2013).
28. M. L. Hu and H. Fan Phys. Rev. A 86, 032338 (2012).
29. M. L. Hu and H. Fan Phys. Rev. A 87, 022314 (2013).
30. D. Wang , A. Huang, F. Ming , W. Sun, H. Lu , C. Liu and L. Ye, Laser Phys. Lett. 14, 065203 (2017).
31. D. Wang , F. Ming , A. J. Huang , W. Y. Sun and L. Ye, Laser Phys. Lett. 14, 095204 (2017).
32. D. Wang , F. Ming , A. J. Huang , W. Y. Sun , J. D. Shi and L. Ye, Laser Phys. Lett. 14, 055205 (2017).
33. A. J. Huang , J. D. Shi , D. Wang and L. Ye, Quantum Inf. Process. 16, 46 (2017).
34. A. J. Huang , D. Wang , J. M. Wang , J. D. Shi , W. Y. Sun and L. Ye, Quantum Inf. Process. 16, 204 (2017).
35. D. Wang , A. J. Huang , R. D. Hoehn , F. Ming , W. Y. Sun , J. D. Shi , L. Ye and S. Kais, Sci. Rep. 7, 1066 (2017).
36. P. F. Chen , W. Y. Sun , F. Ming , A. J. Huang , D. Wang and L. Ye, Laser Phys. Lett. 15, 015206 (2018).
37. M. N. Chen , W. Y. Sun , A. J. Huang , F. Ming , D. Wang and L. Ye, Laser Phys. Lett. 15, 015207 (2018).
38. D. Wang , W. N. Shi , R. D. Hoehn , F. Ming , W. Y. Sun , S. Kais and L. Ye, Ann. Phys. (Berlin) 530, 1800080 (2018).
39. F. Ming , D. Wang , A. J. Huang , W. Y. Sun and L. Ye, Quantum Inf. Process. 17, 9 (2018).
40. Y. Zhang , M. Fang , G. Kang , and Q. Zhou, Quantum Inf. Process. 17, 62 (2018).
41. F. Ming , D. Wang , W. N. Shi , A. J. Huang , W. Y. Sun and L. Ye, Quantum Inf. Process. 17, 89 (2018).
42. Y. N. Guo , M. F. Fang and K. Zeng, Quantum Inf. Process. 17, 187 (2018).
43. J. Q. Li , L. Bai and J. Q. Liang, Quantum Inf. Process. 17, 206 (2018).
44. F. Ming , D. Wang , W. N. Shi , A. J. Huang , M. M. Du , W. Y. Sun and L. Ye, Quantum Inf. Process. 17, 267 (2018).
45. Y. Zhang , Q. Zhou , M. Fang, G. Kang and X. Li, Quantum Inf. Process. 17, 326 (2018).
46. D. Wang , W. N. Shi , R. D. Hoehn , F. Ming , W. Y. Sun , L. Ye and S. Kais, Quantum Inf. Process. 17, 335 (2018).
47. P. F. Chen , L. Ye and D. Wang, Eur. Phys. J. D 73, 108 (2019).
48. W. N. Shi, F. Ming , D. Wang and L. Ye, Quantum Inf. Process. 18, 70 (2019).
49. Y. Y. Yang , W. Y. Sun , W. N. Shi , F. Ming , D. Wang and L. Ye, Front. Phys. 14, 31601 (2019).
50. M. N. Chen , D. Wang and L. Ye, Phys. Lett. A 383, 977 (2019).
51. F. Ming , D. Wang and L. Ye, Ann. Phys. (Berlin) 531, 1900014 (2019).
52. Y. B. Yao , D. Wang , F. Ming and L. Ye, J. Phys. B: At. Mol. Opt. Phys. 53, 035501 (2020).
53. Z. Y. Ding , H. Yang , H. Yuan , D. Wang , J. Yang and L. Ye, Phys. Rev. A 101, 022116 (2020).
54. H. Yang , Z. Y. Ding , D. Wang , H. Yuan , X. K. Song , J. Yang , C. J. Zhang and L. Ye, Phys. Rev. A 101, 022324 (2020).
55. Z. Y. Ding , H. Yang , D. Wang , H. Yuan , J. Yang and L. Ye, Phys. Rev. A 101 032101 (2020)
56. M. R. Pourkarimi, Int. J. Quantum Inform. 16, 1850057 (2018).
57. M. R. Pourkarimi, Int. J. Quantum Inform. 17, 1950008 (2019).
58. Z. Huang, Laser Phys. Lett. 15, 025203 (2018).
59. B. L. Fang , J. Shi and T. Wu, Int. J. Theor. Phys. 59, 763 (2020).
60. S. Haddadi , M. R. Pourkarimi , A. Akhound and M. Ghominejad, Laser Phys. Lett. 16, 095202 (2019)
61. M. R. Pourkarimi and S. Haddadi, Laser Phys. Lett. 17, 025206 (2020).
62. F. Adabi , S. Salimi and S. Haseli, Phys. Rev. A 93, 062123 (2016).

-
63. F. Adabi , S. Salimi and S. Haseli, *Europhys. Lett.* 115, 60004 (2016).
 64. H. Dolatkhah , S. Haseli , S. Salimi and A. S. Khorashad, *Quantum. Inf. Process.* 18, 13 (2019).
 65. S. Haseli , H. Dolatkhah , S. Salimi and A. S. Khorashad, *Laser Phys. Lett.* 16, 045207 (2019).
 66. S. Haseli , H. Dolatkhah , H. Rangani Jahromi , S. Salimi and A. S. Khorashad, *Opt. Commun.* 461, 125287 (2020).
 67. M. H. Partovi, *Phys. Rev. A* 86, 022309 (2012).
 68. Y. Huang, *Phys. Rev. A* 82, 012335 (2010).
 69. R. Prevedel, D. R. Hamel, R. Colbeck, K. Fisher and K. J. Resch, *Nature Phys.* 7, 757 (2011).
 70. L. C. Feng, J. S. Xu, X. Y. Xu, K. Li and G. C. Guo, *Nature Phys.* 7, 752 (2011).
 71. M. Tomamichel, C. C. W. Lim, N. Gisin and R. Renner, *Nature Commun.* 3, 634 (2012).
 72. N. H. Y. Ng, M. Berta and S. Wehner, *Phys. Rev. A* 86, 042315 (2012).
 73. A. K. Ekert, *Phys. Rev. Lett.* 67 661 (1991).
 74. J. M. Renes and J. C. Boileau *Phys. Rev. Lett.* 103 020402 (2009).
 75. I. Devetak and A. Winter, *Proc. R. Soc. A* 461 207 (2005).
 76. J. Feng, Y. Z. Zhang, M. D. Gould, H. Fan, *Phys. Lett. B* 726, 527-532 (2013).
 77. J. Feng, Y. Z. Zhang, M. D. Gould, H. Fan, *Phys. Lett. B* 743, 9 198-204 (2015).
 78. J. L. Huang, W. C. Gan, Y. Xiao, F. W. Shu and M. H. Yung, *Eur. Phys. J. C* 78:545 (2018).
 79. L. Jia, Z. Tian, J. Jing, *Annals of Physics* 353, 37-47 (2015).
 80. I. Fuentes-Schuller, R.B. Mann, *Phys. Rev. Lett.* 95, 120404 (2005).
 81. Q. Pan, J. Jing, *Phys. Rev. D* 78, 065015 (2008).
 82. J. Wang, Q. Pan, J. Jing, *Phys. Lett. B* 692, 202 (2010).
 83. E. Martin-Martinez, L.J. Garay, J. Leon, *Phys. Rev. D* 82, 064006 (2010).
 84. E. Martin-Martinez, J. Leon, *Phys. Rev. A* 81, 032320 (2010).
 85. G.W. Gibbons, S.W. Hawking, *Phys. Rev. D* 15, 2738 (1977).
 86. S.W. Hawking, *Commun. Math. Phys.* 43, 199 (1975).
 87. T. Damour, R. Ruffini, *Phys. Rev. D* 14, 332 (1976).
 88. J. Wang, Q. Pan, J. Jing, *Ann. Phys.* 325, 1190 (2010).
 89. D. Garfinkle, G.T. Horowitz, A. Strominger, *Phys. Rev. D* 43, 3140 (1991).
 90. A. Gareia, D. Galtsov, O. Kechkin, *Phys. Rev. Lett.* 74, 1276 (1995).
 91. Y. Huang, K. Yan, Y. Wu, X. Hao, *Eur. Phys. J. C* 79:974 (2019).
 92. E. Martin-Martinez, L.J. Garay, J. Leon, *Phys. Rev. D* 82, 064006 (2010).
 93. D.E. Bruschi, J. Louko, E. Martin-Martinez, A. Dragan, I. Fuentes, *Phys. Rev. A* 82, 042332 (2010).